

7. On the Crustal Structure in North-East Japan by Explosion Seismic Observations.

By Takeo MATUZAWA,

Geophysical Institute, Faculty of Science, The University of Tôkyô.

(Read Dec. 23, 1958.—Received Dec. 27, 1958.)

1. Prefatory remarks

Several sets of seismic observations were made by our research group for explosion seismology on the occasions of large blasts in North-east Japan. A summarizing report¹⁾ of the investigation of those observations was presented to the Rome Assembly of the I.U.G.G., 1954 under the title "Crustal structure in North-east Japan by explosion seismic observations". In that report broad aspects of our investigations were given but detailed discussions were omitted. In the present paper our precise discussions made in the course of our reductions will be given in order to furnish exact knowledge of the reliability of our results. We shall put forward our statements, referring to the Rome Assembly Report (later reference, R.A.R.). In R.A.R. the romanization of the name of places in Japan was sometimes confused, i.e. the Japanese system and the Hepburn system were mingled. In the present paper the Japanese system is adopted. The romanization of the personal name is of course left to the usage of each person.

The main differences between them are as follows;

Japanese system	Hepburn system	Japanese system	Hepburn system
Hu	Fu	Ti	Chi
Si	Shi	Tu	Tsu
Sya	Sha	Tya	Cha
Syu	Shu	Tyu	Chu
Syo	Sho	Tyo	Cho
Zi	Ji	An	Am
Zya	Ja	In	Im
Zyu	Ju	Un	Um
Zyo	Jo	En	Em
		On	Om

before b,
p and m.

1) Research group for explosion seismology (Japan), *Pub. Bureau Central Séism. Intern. Série A. Trav. Sci. Fasc.*, **19** (1954), 229-242.

In the Japanese system a circonflex is put on a vowel, which should be pronounced somewhat long, for example, Tôkyô in stead of Tokyo or Tokio in the Hepburn system.

Members of the group, who participated in this reduction and discussion, were, in the alphabetical order, T. Asada, S. Asano, N. Den, T. Kaneko, K. Kasahara, H. Kawasumi, N. Kobayashi, T. Matsumoto, T. Matuzawa, T. Mikumo, S. Miyamura, S. Murauti, A. Okada, S. Omote, E. Shima, S. Suyehiro, Z. Suzuki, A. Takagi, I. Tamaki and T. Usami. Voluminous and tedious reductions for the crustal structure were carried out for the most part by N. Den and Z. Suzuki.

Detailed descriptions of observation points, blasts, instruments, observers, etc. in English were reported in the following publications.

Blast	Publication
I. 1	Bull. Earthq. Res. Inst., 29 (1951), p. 97.
I. 2	30 (1952), p. 279.
I. 3	31 (1953), p. 281.
K.1	32 (1954), p. 79.
K.2	33 (1955), p. 693.

2. Determination of the shot times of both the Isibuti 1 and Isibuti 2 blasts

In order to construct synthetical travel time curves from several sets of observations of blasts, it was necessary to know the accurate time of each blast, because each set had very few, if any, common observation points, and the precise position of each shot was not the same. At the first two Isibuti blasts the shot times were not marked on the seismogram. We determined them as follows.

The Data of travel times for I.1, I.2 and I.3 blasts are given in Table 1.

These values are plotted in Fig. 1.

For I.3, putting $T=a\Delta$, we obtain by the method of least squares $1/a(\text{velocity})=2.51 \pm 0.052 \text{ km/sec}$.

For I.2, putting $T=a\Delta+b$, we get the same value of a and the shot time $12^{\text{h}}05^{\text{m}}59.82^{\text{s}}$.

For I.1, assuming the same value of a , we get $12^{\text{h}}06^{\text{m}}07.64^{\text{s}}$ as the shot time, which is different by 0.33 sec from the value, deduced from remote observations. Of course this shot time should be adopted.

Table 1.

Blast	Station	Epicentral distance (km)	travel time (sec)	shot time
I.1 ²⁾	Isibuti	1.69	0.67	12 ^h 06 ^m 07.97 ^s deduced from arrival times within 4 km.
I.2	Tunnel 1	0.24	0.088	12 ^h 05 ^m 59.84 ^s deduced from arrival times within 5 km.
	Tunnel 2	0.33	0.127	
	Orose	1.08	0.43	
	Isibuti	1.69	0.68	
I.3	Tunnel 1	0.22	0.05	12 ^h 04 ^m 59.42 ^s . Shot time marked on the seismogram.
	Tunnel 2	0.31	0.09	
	A	1.50	0.60	
	B	1.73	0.69	

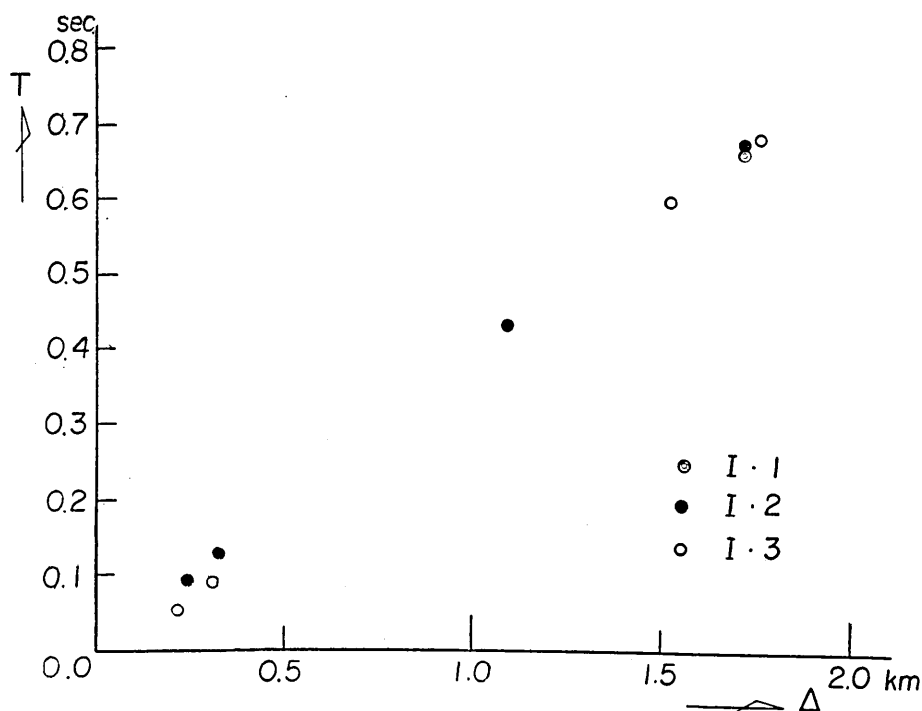


Fig. 1.

2) The longitude of the Isibuti shot point I.1 must be 140°53'37''E instead of 140°51'37''E printed in Table 1 in Report I.1.

3. The *P*-wave velocity in the uppermost layer near shot points

(i) Near Isibuti shot points.

As stated in 2, the *P*-wave velocity in the uppermost layer near Isibuti shot points is 2.51 km/sec, because its intercept time is zero.

(ii) Near Kamaisi shot points.

Travel times near shot points K.1 and K.2 were observed, and they are shown in Fig. 2 and tabulated in Table 2.

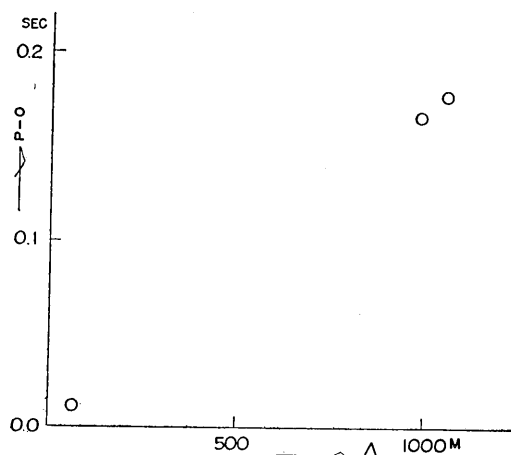


Fig. 2.

Table 2.

Δ in m	6.5	989	1055
$P-O$ in sec	0.011	0.166	0.177

The error of the travel time in the observation is limited within 0.002~0.003 sec.

The accuracy of the epicentral distance Δ did not match to that of the time measurement and was somewhat lower. Blast chambers were complicately located in

the mine, however, these were minutely shown in a map of the mine. Positions of the observation points were also determined on a map outside the mine. But a map connecting both maps was found somewhat inaccurate, and errors of a few tens of meters in the epicentral distance are liable to creep in.

From Fig. 2 the velocity of the *P* wave is calculated as 6.0 km/sec with practically zero intercept time, however, owing to the above stated uncertainty in Δ , range of uncertainty about 0.2 km/sec in the velocity must be allowed.

At any rate, it is certain that near Kamaisi shot points a layer with *P*-wave velocity about 6.0 km/sec is exposed practically to the surface.

4. Synthetical travel times and their accuracy

Taking these precautions, synthetical travel times were obtained as tabulated in Table 3 and also given in R.A.R.

Table 3.

Blast	Station	distance km	azimuth from N over E	travel time T in sec	$T - \frac{d}{6}$
Isibuti South (IS) profile					
I.3		2.70	182°	0.95	0.50
I.2	Hondera	15.3	166	2.96	0.41
I.3	"	"	"	3.02	0.47
I.2	Kurikoma	22.5	175	4.17	0.42
I.3	Hosokura	32.2	180	5.85	0.46
I.1	Hanaizumi	38.5	141	6.83	0.43
I.2	Kawatabi	41.9	196	7.61	0.63
I.3	"	"	"	7.59	0.61
I.1*	Matusima	81.4	169	14.59	1.02
I.2*	"	"	"	14.68	1.08
I.3	Nenosiroisi	87.8	185	15.24	0.61
I.1	Sendai	98.2	102	16.86	0.43
I.1*	Watari	119.4	180	20.03	0.14
I.3	Daiyama	148.8	197	25.07	0.27
I.2	Sinobu	159.9	194	26.75	0.10
I.3	Hatori	216.4	199	34.6	-1.47
I.3*	Motegi	290.7	193	44.50	-3.95
I.3	Tukuba	327.1	192	50.2	-4.32
Isibuti West (IW) profile					
I.3	Katurazawa	22.20	241	4.41	0.71
I.3	Yuzawa	33.77	280	6.31	0.68
I.3	Innai	45.98	262	8.56	0.90
I.3*	Mamurogawa	58.72	243	10.74	0.95
I.3	Sinasawa	89.99	238	16.04	1.04
Isibuti East (IE) profile					
I.2	Umadome 1	4.31	69	1.36	0.64
I.2	Umadome 2	4.40	"	1.39	0.66
I.2	Atago	8.65	78	2.38	0.94
I.2	Dobasi	12.09	83	3.08	1.07
I.2	Wakayanagi	14.62	80	3.21	0.77
I.1	"	15.06	"	3.16	0.65
I.2	Mizusawa	21.10	83	4.11	0.59
I.1	Maesawa	21.24	110	4.40	0.87
I.2	Setamai	55.90	86	9.97	0.65
I.2*	Kamaisi	87.54	80	14.84	0.25

(to be continued)

Table 3.

(continued)

Blast	Station	distance km	azimuth from N over E	travel time T in sec	$T - \frac{d}{6}$
Kamaisi South (KS) profile					
K.2	Nakasone	11.1	203	2.03	0.18
K.1	Setamai	20.6	222	3.60	0.17
K.2	Sakari	23.8	182	4.08	0.11
K.1	Kesennuma	45.8	194	7.72	0.09
K.2	"	45.6	"	7.58	-0.02
K.2	Sizugawa	72.2	197	11.96	-0.07
K.1*	Onagawa	97.6	193	15.92	-0.25
K.2	"	97.4	"	16.03	-0.20
K.2	Mukaiyama	137.3	211	22.93	0.05
K.2	Hunaoka	159.6	209	26.00	-0.60
K.1*	Kaneyama	173.9	207	28.28	-0.70
K.2	"	173.6	"	28.13	-0.84
K.1	Kawamata	202.5	209	31.84	-1.94
K.2	"	202.4	"	31.82	-1.91
K.1	Siroisi	226.0	208	35.35	-2.32
K.2	"	225.9	"	35.31	-2.34
K.1	Nogisawa	261.2	206	39.09	-4.44
K.2	"	260.9	"	40.0	-3.48
K.2	Motegi	331.5	201	49.0	-6.25
Kamaisi West (KW) profile					
K.2	Umanokiuti	4.82	263	0.90	0.10
K.1	Ide	37.1	248	6.39	0.21
K.1	Mizusawa	51.6	250	9.09	0.49
K.1*	Yuzawa	103.5	262	18.13	0.88
K.1	Mamurogawa	130.7	248	22.66	0.88

Data marked with an asterisk * are those, which were corrected in this study and somewhat different from those in other reports.

5. Accuracy of the data

The accuracy of a crustal structure deduced from the observed travel times depends on the accuracy of the data. Therefore, it is important to ensure the accuracy of the latter. Sources of time errors in the travel time are classified as follows:

1. Errors of identification of the commencement of the wave.
2. Errors of time measurements on the record.

3. Irregularities due to the weathered layer.

As to (1), the identification was made by several persons independently, and readings were accepted only when satisfactory agreement was found. Errors of this category are expected to be very small, except for stations at very remote epicentral distances.

As to (2), the maximum error is expected not to exceed 0.1 sec. At most of the observation points, the running speed of the recording paper is 2~3 cm per second or more, and moreover second and minute marks are put directly from the JJY radio time signal. Therefore, the error of time measurement does not exceed 2 or 3 hundredths of a second. At stations very near to the shot point time marks of one hundredth of a second are put, so that accuracy of 2 or 3 thousandths of a second is secured. At some stations, where the JJY reception failed, the time was determined from chronometers, and the error is expected not to exceed 0.1 sec.

As to (3) this is not due to observations, however, it is very local, and in this paper it is treated as a sort of errors. A layer of 2.51 km/sec is accepted as the surface layer, and any local weathered layer other than this one comes under this category. Most observation points were selected in such a way that instruments could be put in caves of the bed rock. From the geological point of view and some trial computations, it was found that the error due to this factor cannot be more than 0.1 sec.

In the next place, the accuracy of the determination of the position of observation and shot points must come under consideration. In the present sets of observations, the positions were identified on the topographical map on a scale of 1/50000 issued by the Geographical Institute, Japan. Hence the error of the relative distance between a shot point and an observation point is expected not to exceed 100 m at most. Therefore, the accuracy of the space determination matches the time accuracy well.

Considering these factors, the total amount of the error is estimated to be less than 0.1 second. In other words, if a fluctuation in travel times exceeds 0.1 sec, the amount must be significant and taken into account in our study.

6. General consideration to the travel time diagram

From the synthetical travel times in Table 3, a travel time diagram as shown in Fig. 3 is obtained.

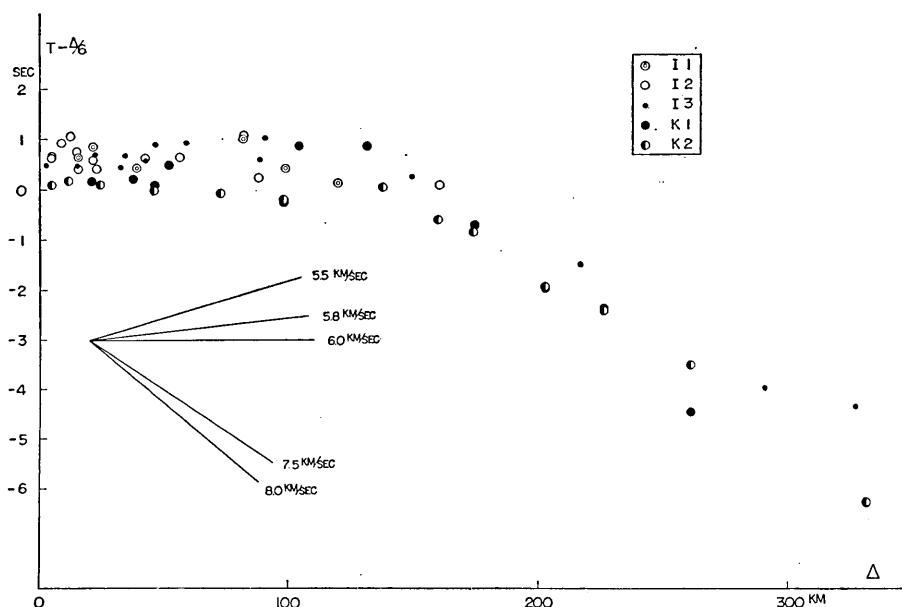


Fig. 3.

Though the plotted points are confined within about 1 sec as far as 150 km, the scatter exceeds far beyond the limit of error already stated, i.e. 0.1 sec. If we classify the points according to the azimuth of the station relative to the shot point, certain systematic deviations are found. This fact suggests that a certain boundary or boundaries of different geological layers are inclined to the horizontal plane with certain dips and strikes.

In deducing the underground structure, we adopt the following guiding principles.

(1) As the first step, seismological data only are used for the interpretation of the crustal structure.

Geological or gravity data are taken into account only to check whether the interpretation is adequate or not.

(2) The proposed model must be as simple a one as possible, that means, a model with the least number of possible assumptions necessary to explain the observed data.

As a natural consequence, a constant velocity of the seismic wave is assumed at least as a first approximation in a certain specified layer.

Under these restrictions a few cases of observed anomalies remain unexplained. These cases are mainly due to the lack of sufficient data in the neighbourhood of the point in question.

7. Discussions on the mode of stratifications of various layers

We can distinguish 4 distinct layers P_1 , P_2 , P_3 and P_4 specified by velocities of the P waves, i.e. 2.51 km/sec for P_1 , 5.75~5.85 km/sec for P_2 , 6.1~6.2 km/sec for P_3 and 7.5~8.0 km/sec for P_4 .

We will discuss the form of each layer as precisely as possible on the basis of travel time curves which were also given both in tables and figures in R.A.R. Abbreviations for profiles here used are the same as those given in that report. For instance, IE stands for the eastern profile of the Isibuti explosion.

8. Remarks on travel times in each profile

(i) *IE profile* (Fig. 4). As stated in section 2, for $\Delta < 2$ km travel times are almost exactly on a straight line, giving 2.51 km/sec. In the domain $2.7 < \Delta < 12$ km they are on a straight line, showing an apparent velocity 4.4 km/sec, and for $\Delta > 14$ km they are scattered around a

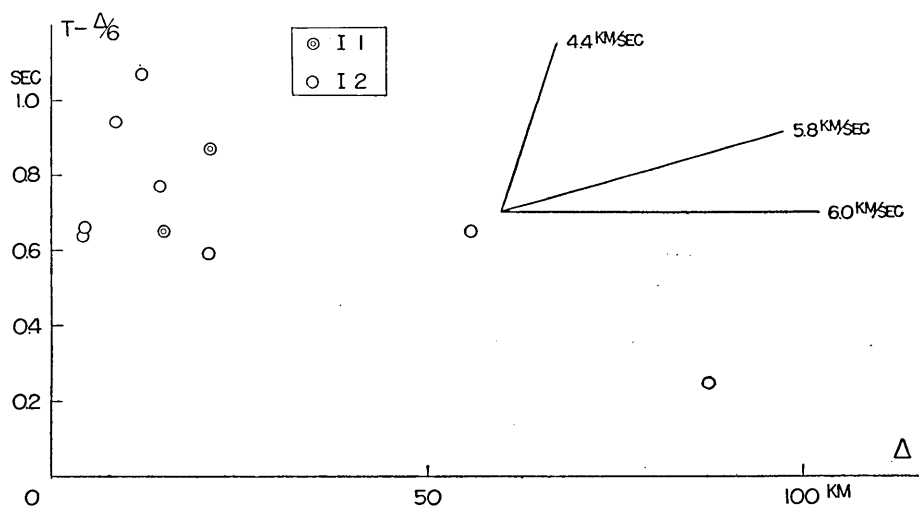


Fig. 4.

straight line, giving approximate velocity 5.8~6.0 km/sec. In the neighbourhood of $\Delta = 14$ km, i.e. between Dobasi station and Wakayanagi station, a gap of travel time, amounting to 0.4~0.6 sec, is seen, and the travel time belonging to the remoter branch, i.e. $\Delta > 14$ km, appears earlier.

(ii) *IW profile* (Fig. 5). Travel times are scattered around a straight line with the intercept time 0.1 sec, giving velocity 5.5~5.8 km/sec.

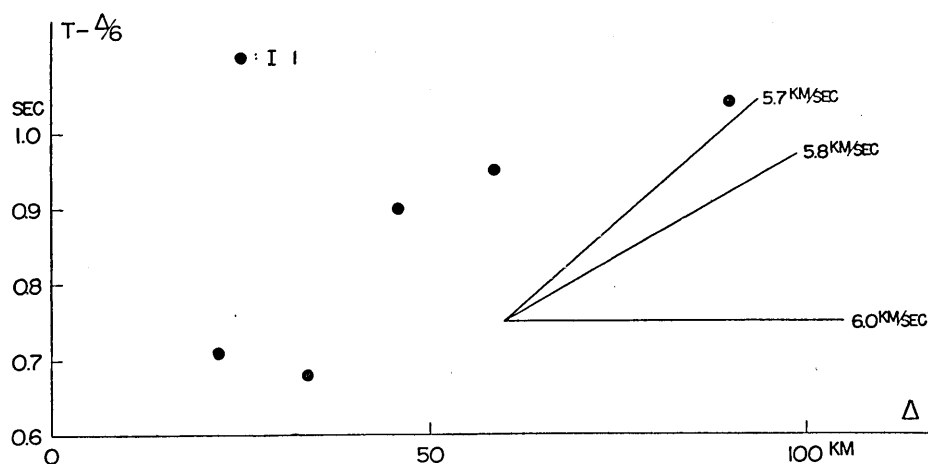


Fig. 5.

(iii) *KW profile* (Fig. 6). Travel times are scattered around a straight line with the intercept time 0.1 sec, giving velocity 5.7~5.8 km/sec.

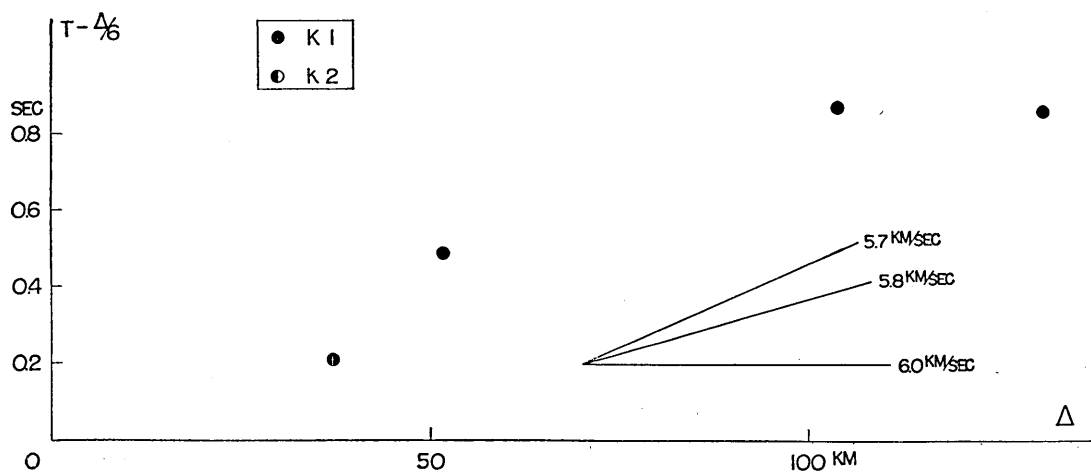


Fig. 6.

(iv) *IS profile* (Fig. 7). For $\Delta < 40$ km travel times are on a straight line with the intercept time $0.2 \sim 0.4$ sec, giving velocity $5.7 \sim 6.0$ km/sec. For $40 < \Delta < 150$ km, we can fit a straight line with intercept time $1.0 \sim 2.0$ sec, giving velocity $6.1 \sim 6.3$ km/sec. Travel times fluctuate rather remarkably, though the range of fluctuation is confined within 1 sec. It seems probable that crustal domains specified by these 3 velocities would have a stratified structure bounded by discontinuity surfaces.

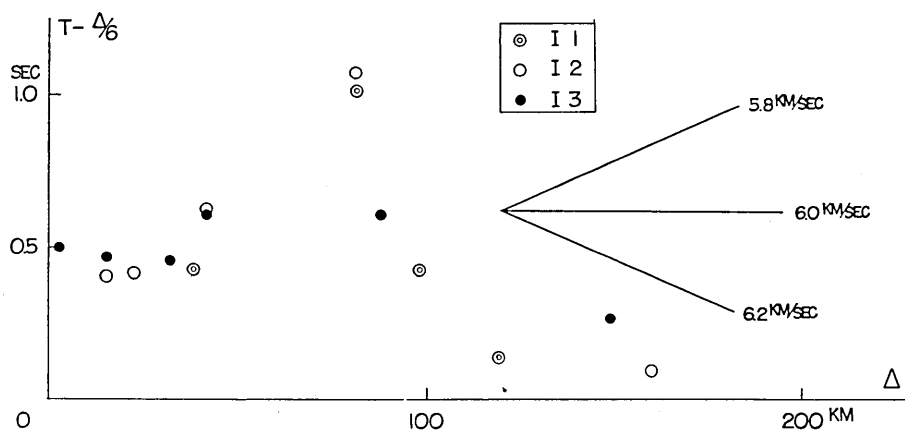


Fig. 7.

(v) *KS profile* (Fig. 8). Within 20 km points are on a straight line with intercept time 0.1 sec, giving velocity $5.7 \sim 6.0$ km/sec. For

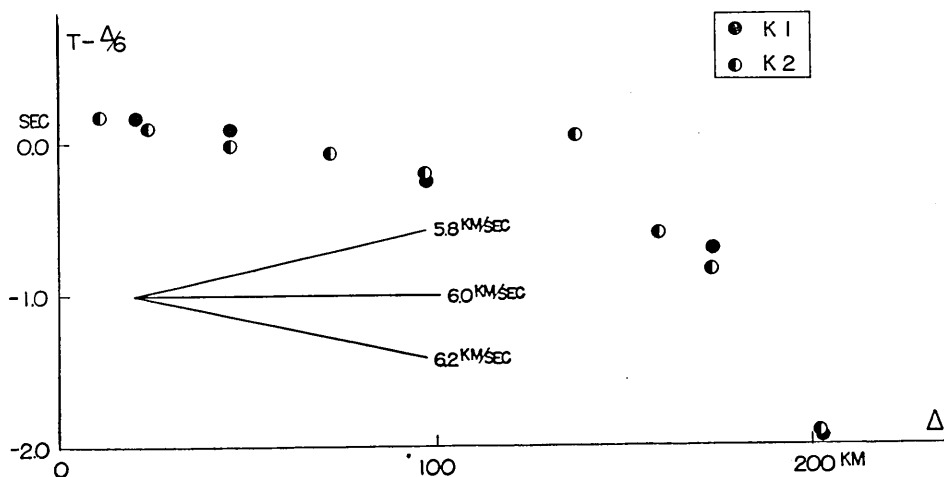


Fig. 8.

$20 < \Delta < 160$ km, points are scattered around a straight line with intercept time 0.5 sec, giving velocity 6.1~6.3 km/sec. From remoter places the velocity is estimated to 7.5~8.0 km/sec.

In this case also we can infer 3 layers with different velocities. Outlines of the crustal structure deduced from these results are summarized in R.A.R.

Now we proceed to the discussion of the form of each layer.

9. Form of the P_1 layer

(i) *Discussion of travel times which give the velocity 4.42 km/sec (Refer to Fig. 9 in R.A.R.)*

This velocity is found only in the IE profile and the travel time is given by a straight line $T = \Delta/4.42 + 0.38$ (T in sec, Δ in km).

If we assume existence of this layer, the crustal model near Isibuti should be as shown in Fig. 9 (A) in R.A.R. Inclination, thickness, etc. of this layer were so determined that they should give, additionally to the IE profile, travel times reconcilable to those both for the KW and IW profile.

If we discard existence of this layer, we must take a crustal model as shown in Fig. 9 (B) in R.A.R. Inclination θ and depth under Isibuti are calculated as $8^\circ \sim 10^\circ$ and 530 m from travel times in the IE profile. In model (B) if we construct a graph for θ and h , taking the velocity in

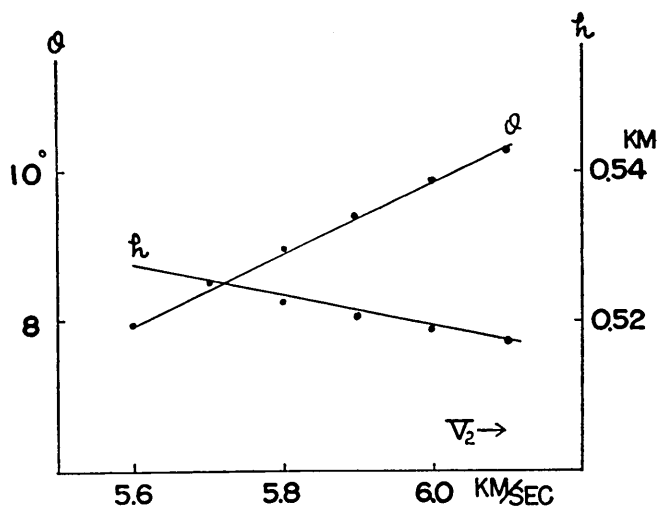


Fig. 9.

the lower layer V_2 as abscissa, we obtain Fig. 9.

It should be remarked that h varies slowly with V_2 .

On the other hand, the intercept time of the line giving velocity 5.8 km/sec in the IS profile is 0.3~0.4 sec as shown before.

Assuming that the form of the cross section is invariable in the NS direction both for the (A) and (B) models, we can calculate the intercept times for both models. That for model (A) should be 0.7 sec and 0.36 sec for model (B).

Thus we conclude that the velocity 4.42 km/sec is nothing but an apparent one and should be discarded.

Ultimately, we adopt 4 layers as shown in section 7.

(ii) *Form of the P_1 layer in the IE profile*

Model (B) holds to a distance somewhere between Dobasi and Wakayanagi, namely 14 km ca., because, as shown in section 8 (i), there is a discontinuity of the travel time. We suppose that the P_1 layer ceases to exist there, say at a distance x_0 from Isibuti (Fig. 10).

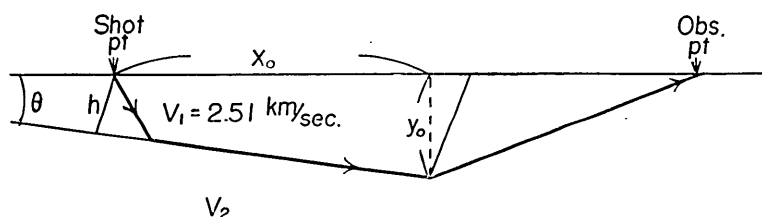


Fig. 10.

Beyond x_0 , diffracted waves whose path is shown in Fig. 10, would be observed. Taking x_0 and V_2 as parameters, residues of travel times i.e. $T_0 - T_c$ at some stations are tabulated in Table 4.

For Kamaisi, a remoter station, the path of the wave, which is ex-

Table 4.

Station \ V_2	x_0 13 km				14 km			
	5.60	5.70	5.80	5.90	5.60	5.70	5.80	5.90
Wakayanagi I	0.17	0.18	0.22	0.26	0.02	0.05	0.08	0.12
Wakayanagi II	0.04	0.08	0.12	0.16	-0.05	-0.02	0.01	0.05
Mizusawa	0.04	0.12	0.13	0.24	0.03	0.10	0.15	0.22
Setamai	0.26	-0.08	0.09	0.26	-0.28	-0.08	0.09	0.26

pected to arrive there at first, should lie in the P_3 layer. In the above calculation we assume that the P_2 layer is exposed to the surface beyond x_0 . The effect of the weathered layer tends to make T_0 late and the judgement of the onset time of the initial motion has also a retarding tendency. Therefore, if the model is a true one and the above mentioned two effects are the only causes of uncertainties, a negative value of $T_0 - T_c$ is improbable.

After all, within our criterion of accuracy, x_0 is 14 km with an uncertainty within 1 km and V_2 is 5.75~5.85 km/sec. The residue at Mizusawa is 0.10~0.20 sec and somewhat large compared with other stations. Hence, at Mizusawa the P_2 layer is probably covered by a certain thin surface layer. If it is the P_1 layer, its thickness is estimated to 300~500 m.

(iii) *Form of the P_1 layer in the IW profile*

If the P_2 layer is exposed to the surface in the further west, the expected travel times are shown by full lines in Fig. 11, taking V_2 as the parameter. Dots are observed points.

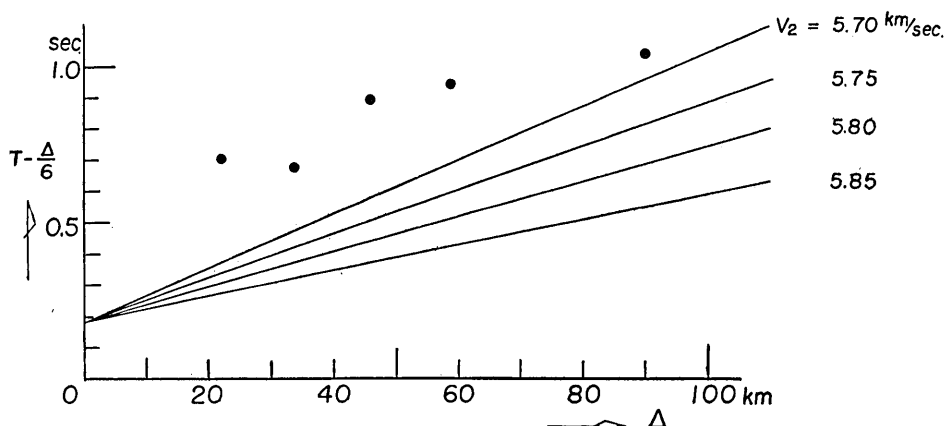


Fig. 11.

As apparent from the figure, observed travel times are systematically much later than the calculated values. Therefore, there should be a certain surface layer on the P_2 layer. As for this surface layer, we have no sufficient data to estimate its velocity. The western extension of the P_1 layer under Isibuti must end at 3 km from Isibuti, if we prolong its lower boundary to the west. Hence, there is no gua-

rantee for taking this layer to be the same one as the P_1 layer.

If we assume the existence of the P_1 layer in the western extension, its thickness can be calculated. Taking V_2 as the parameter, retardation δT of the travel time due to this layer, and the corresponding thickness of the layer, Z , are tabulated in Table 5.

Table 5.

Station \ V_2	δT				Z			
	5.75	5.80	5.85	5.90	5.75	5.80	5.85	5.90
Katurazawa	0.36	0.40	0.43	0.47	1.0	1.1	1.2	1.3
Yuzawa	0.25	0.31	0.36	0.41	0.70	0.86	1.0	1.1
Innai	0.38	0.46	0.53	0.60	1.1	1.3	1.5	1.7
Mamurogawa	0.34	0.43	0.52	0.61	0.95	1.2	1.4	1.7
Sinasawa	0.20	0.34	0.48	0.62	0.56	0.94	1.3	1.7

Comparing δT with the plot in Fig. 11, we see that 5.80 km/sec for V_2 is most compatible.

(iv) *Form of the P_1 layer in the KW profile*

As stated before, we can assume practically that the P_2 layer is exposed to the surface near Kamaisi shot point. Under this assumption, the calculated value $T_0 - T_c$ is tabulated in Table 6.

Table 6.

Station \ V_2	5.75	5.80	5.85	5.90
Umanokiuti	0.06	0.07	0.07	0.08
Ide	-0.6	0.01	0.05	0.11
Mizusawa	0.11	0.19	0.27	0.35

There remains some possibility that the initial pulse observed at Ide or Mizusawa might pass through the P_2 layer. We cannot ascertain this point at present, because the accuracy of determination of the P_3 layer is not sufficient for this purpose.

Here a remark should be added to the travel time at Umanokiuti. At this station we aimed mainly at the observation of reflected waves, and 11 pick-ups were arranged on a nearly straight line. The shot time was marked with the direct connection to the shot point, and the time

mark was put at intervals of 1/100 sec. Travel times at these 11 points are plotted in Fig. 12.

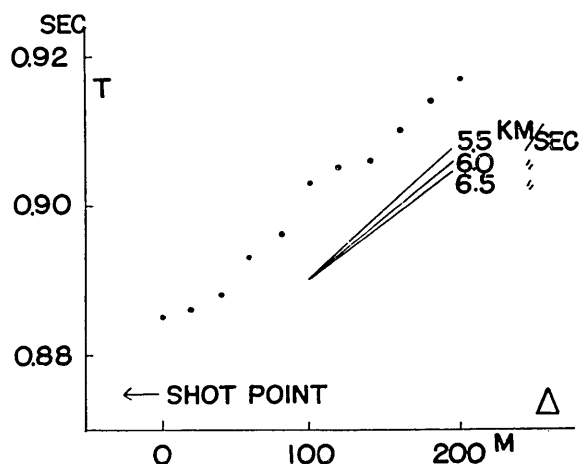


Fig. 12.

are plotted in Fig. 12.

The apparent velocity deduced from this travel time curve is nearly the same as V_z . The travel time and epicentral distance adopted for calculating Table 6 are mean values of these 11 points.

The residue, $T_0 - T_c = 7/100$ sec, reveals the existence of a certain superficial layer, but we have no data for determining its velocity.

(v) *Summary of the study of the form of the P_1 layer in the E-W profile*

Summarizing the results obtained from the IE, IW and KW profiles, we obtain a probable profile of the P_1 layer in the E-W vertical section as shown in Fig. 29.

(vi) *Some considerations on late phases*

At some stations we can distinguish a distinct late phase corresponding to P waves passing exclusively through the P_1 layer. The observed and calculated travel times are shown in Table 7.

Table 7.

Profile	Station	Δ km	T_0 sec	T_c sec
IE	Umadome	4.40	1.74	1.57
"	Dobasi	12.09	4.70	4.64
IS	Kawatabi	41.9	16.8	16.51

T_0 is always a little larger than T_c . This is probably due to the missing of the very commencement of the said phase in reading the seismogram. In the IE profile we cannot find a corresponding phase at stations beyond Dobasi. In the IW profile we cannot find it anywhere.

These facts are quite compatible with our cross section in the E-W profile. In the IS profile, the corresponding late phase is not distinctly discernible beyond Kawatabi. It may be too hasty, however, to deny the existence of the P_1 layer in the southern extension, because we do not know the exact form of the P_1 layer in the KW profile in the southern part.

10. Form of the lower boundary of the P_2 layer

Our process of analysis was briefly given in R.A.R. We will proceed to detailed discussions.

(i) Travel time for an inclined layer boundary

As stated in section 8, as for V_3 (6.1~6.3 km/sec) waves, the intercept time for the Isibuti shots is considerably larger than that for the Kamaisi shots, and the epicentral distance of the intersection with the V_2 curve is also larger for Isibuti shots than for Kamaisi shots. These facts reveal that the depth of the lower boundary of the P_2 layer may be deeper under Isibuti than under Kamaisi, i.e. the boundary is inclined with a certain dip and strike. The relation between shot point O , station P , dip θ , strike θ_0 , azimuth of OP , θ , etc. is shown in Fig. 10 in R.A.R.³⁾ θ_0 and θ are measured from the north over the east.

The travel time for waves passing through the lower layer is given by

$$T = \frac{2h \cos i}{V_2} + \frac{\Delta \sin (i + \theta')}{V_2},$$

where

$$\sin i = V_2/V_3 \quad \text{and} \quad \sin \theta' = \sin \theta \cdot \sin (\theta - \theta_0).$$

θ' is the apparent dip of the boundary in the direction OP , i.e. in the plane including OP and perpendicular to the boundary.

If θ is small and small terms higher than θ^2 are neglected, we obtain

$$T = \frac{2h \cos i}{V_2} + \frac{\Delta}{V_3} + a\Delta \sin (\theta - \theta_0),$$

where

$$a = \theta/V_3 \tan i.$$

3) In the text of R.A.R., H_0 and H are written for θ_0 and θ_1 .

The third term on the right hand side represents the effect of the dip of the boundary. When θ has small fluctuations around θ_0 , corresponding fluctuations appear in the travel time T , or $T - (\Delta/V_3)$.

When the P_2 layer is covered by a thin superficial layer P_1 the following reduction δT for the travel time is necessary in order to apply the above equation directly. Referring to Fig. 13,

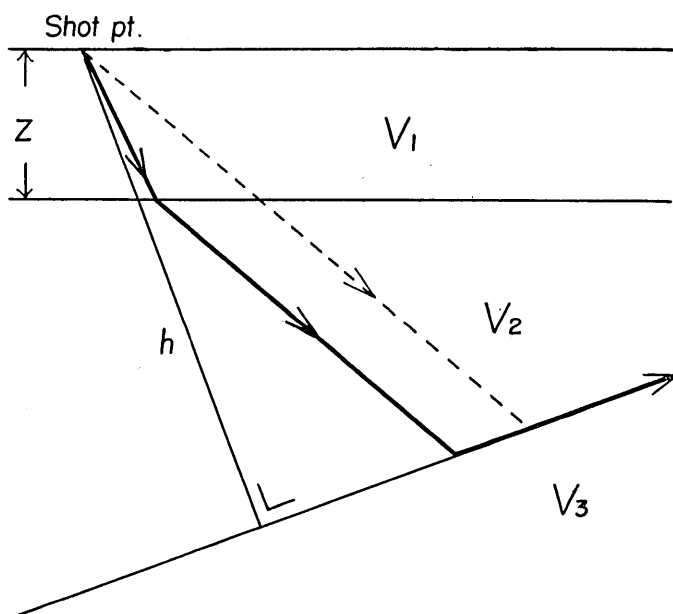


Fig. 13.

$$\frac{\delta T}{Z} = \frac{\tan(i_2 + \theta') - \tan i_1}{\cos i_2} \left\{ \frac{\cos(i_2 + \theta')}{V_3} + \frac{\sin \theta'}{V_2} \right\} + \frac{1}{V_1 \cos i_1} - \frac{1}{V_2 \cos(i_2 + \theta')},$$

where

$$\sin i_1 = V_1/V_2, \quad \sin i_2 = V_2/V_3, \quad \sin \theta' = \sin \theta \cdot \sin(\theta - \theta_0).$$

(ii) *Comparison of the fluctuation of the travel time with $\Delta \sin(\theta - \theta_0)$*

Taking V_3 and θ_0 as parameters, we get graphs for $\Delta \sim T - (\Delta/V_3)$ and $\Delta \sim \Delta \sin(\theta - \theta_0)$ in each profile. Figs. 14, 15, and 16.

In these figs, stations, where the first wave does not pass probably through the P_3 layer, are omitted. In the KW profile, the reduction for the superficial layer is applied. In other profiles, it is omitted, as the true superficial layer is not known for certain.

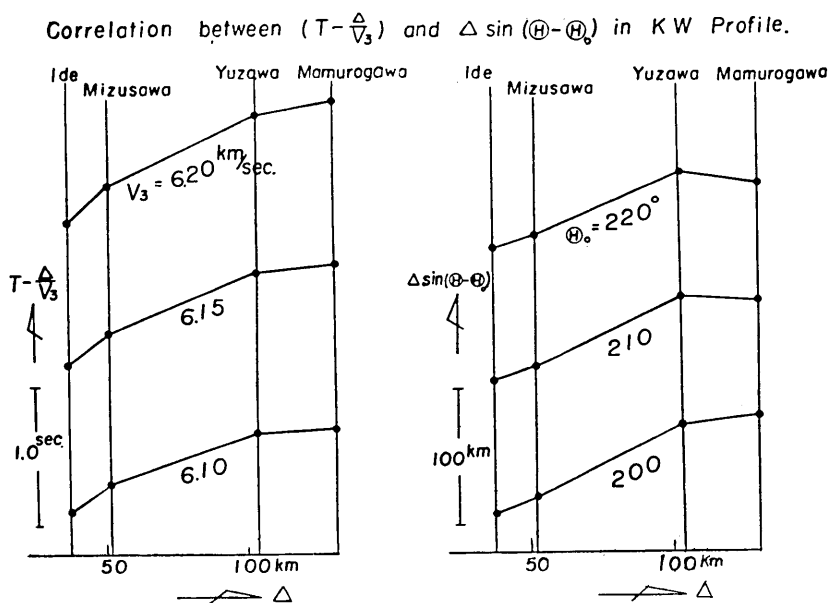


Fig. 14.

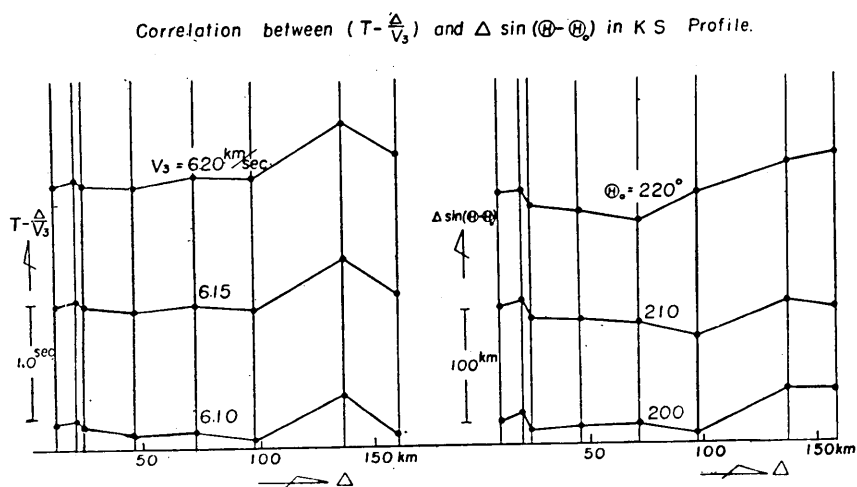


Fig. 15.

In these figs. we can find remarkable correlations between $T - (\Delta/V_3)$ and $\Delta \sin(\theta - \theta_0)$. In other words, we can conclude that the boundary between layer P_2 and layer P_3 in each profile is an inclined plane. In the next place, we must discuss, whether the dip, strike, and V_3 are

Correlation between $(T - \frac{\Delta}{V_3})$ and $\Delta \sin(\Theta - \Theta_0)$ in IS Profile.

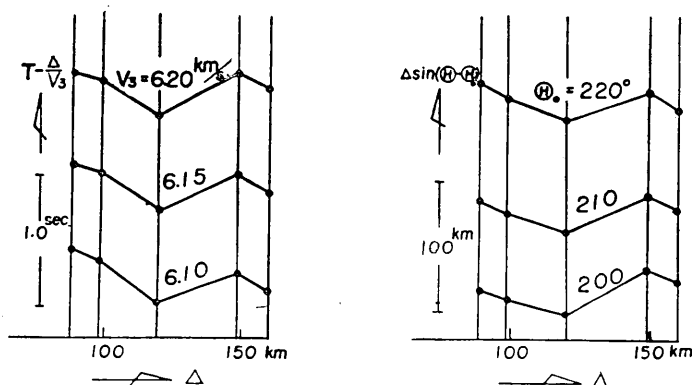


Fig. 16.

common to all profiles or not.

It is not appropriate to apply the method of least squares unconditionally to the result shown in Figs. 14, 15 and 16, because there are many individual uncertainties inherent in each profile, such as effects due to superficial layers etc. After all, we must resort to the method of trial and error for various models and determine the limit of allowance for values of various parameters.

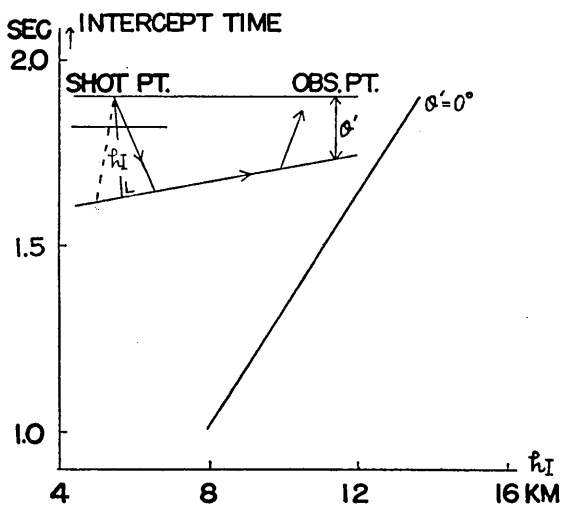


Fig. 17.

(iii) *On the intercept time*

In (i) the effect of a local superficial layer, say the P_1 layer, is omitted. Therefore, the intercept time was constant for all azimuths. As stated in section 9, under the shot point at Isibuti there is a surface layer P_1 . This fact must be taken into account. For the IE profile, the path through the P_3 layer and the relation between the intercept time and h_1 , i.e.

the depth of the P_2P_3 boundary under Isibuti are shown in Fig. 17. Here θ' is taken as the parameter.

As for the IS profile, the effect of the P_1 layer is practically invariable for all stations, because the range of the fluctuation of θ is not large. For the Kamaisi shot point we must take the height of the shot point (500 m) into account. When the shot point has a height above the reference surface, the relation

between the intercept time and h_k , i.e. depth of the layer boundary below the mean sea level under the Kamaisi shot point is shown in Fig. 18, taking θ' as the parameter.

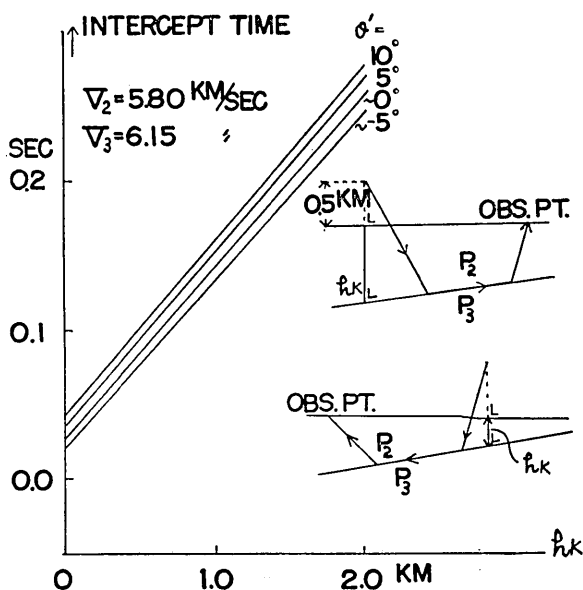


Fig. 18.

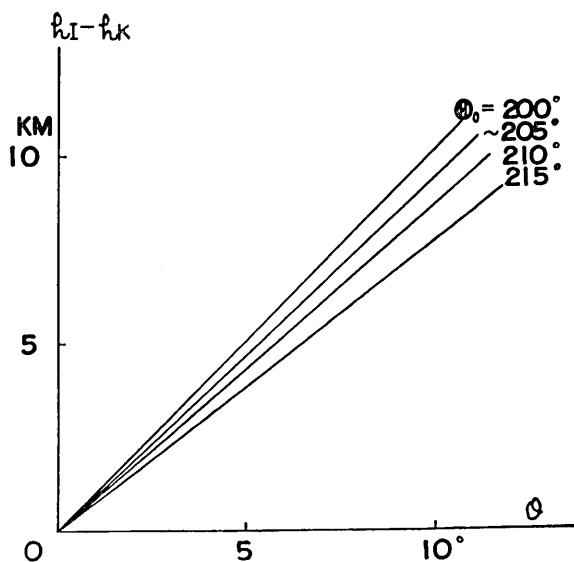


Fig. 19.

From observed travel times, the intercept time for the Isibuti shot is estimated at 1.0~1.6 sec, and that for the Kamaisi shot at 0.1~0.03 sec. From these values we get the range of allowance of the values h_1 and h_k . If the boundary is on one plane, taking θ_0 as the parameter, $h_1 - h_k$ can be calculated geometrically for θ . The result is shown in Fig. 19.

Within the limit of allowance of $h_1 - h_k$ and θ_0 , the corresponding limit

of allowance of θ is within $4^\circ \sim 11^\circ$.

(iv) *In the KW profile*

In the KW profile thickness of the surface layer at each stations was calculated in section 9. Therefore, δT due to this layer can be calculated, as shown in (i). For instance, taking $V_3 = 6.20$ km/sec, δT for various tentative V_2 is given in Table 8.

Table 8.

V_2 \ Station	Mizusawa	Yuzawa	Mamurogawa
5.75 km/sec	0.10 sec	0.21 sec	0.28 sec
5.80	0.12	0.26	0.36
5.85	0.17	0.30	0.42

Applying these corrections and using the formula given in section 10 (i), one of 5 parameters h_k , θ_0 , θ , V_3 , V_2 can be calculated, if any four

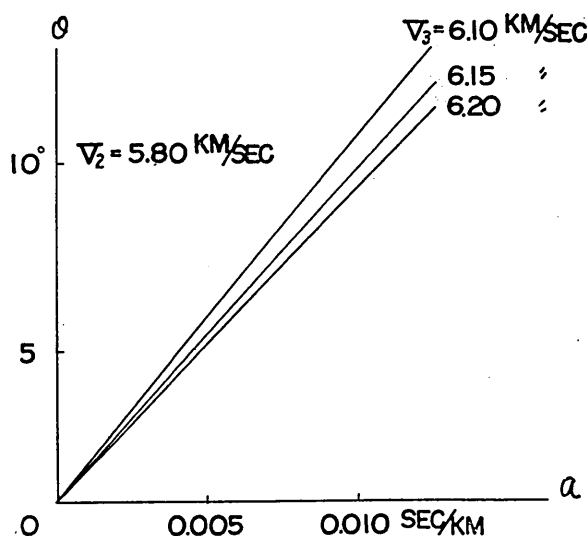


Fig. 20.

of them are given. It is simplest to calculate θ as an unknown. Taking $V_2 = 5.80$ km/sec and V_3 as the parameter, the relation between θ and α is shown in Fig. 20.

Taking the limit of error for the determination of the incident time of the initial phase as 0.1 sec and adopting $\theta_0 = 210^\circ$, $h_k = 1.0$ km, $V_2 = 5.80$ km/sec and $V_3 = 6.15$ km/sec, the limit of allowance of θ at each station is given in Fig. 21.

We see that the com-

mon range for all stations lies around 10° .

(v) *In the IS profile*

In the IS profile the exact form of the P_1 layer is not certain. If we calculate the value of θ on the basis of observed T , and if the P_1

Values of θ Obtained by the Observations
in KW Line

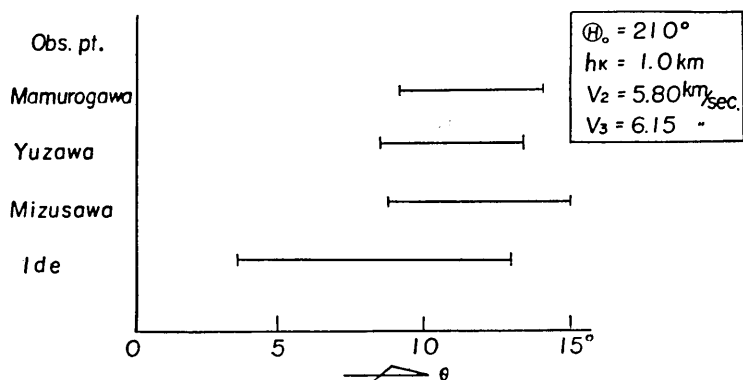


Fig. 21.

layer is absent, it comes out too large compared with that for the existence of the P_1 layer, because T_0 is larger for the existence of the P_1 layer than for its absence.

For instance, taking $\theta_0 = 215^\circ$, $h_k = 1.0 \text{ km}$, $V_2 = 5.80 \text{ km/sec}$ and $V_3 = 6.15 \text{ km/sec}$, $T_0 - T_c$ and θ relation is shown in Fig. 22.

From the above reasoning, $T_0 - T_c$ is expected to be positive within the limit of accuracy 0.1 sec.

(vi) In the IE profile

In this profile only Kamaisi station comes in the scope of our discussion, concerning the P_3 layer. Then two cases are taken into consideration.

(a) Kamaisi station is situated on the P_2 layer.

(b) It lies directly on the P_3 layer or at least the shallowest posi-

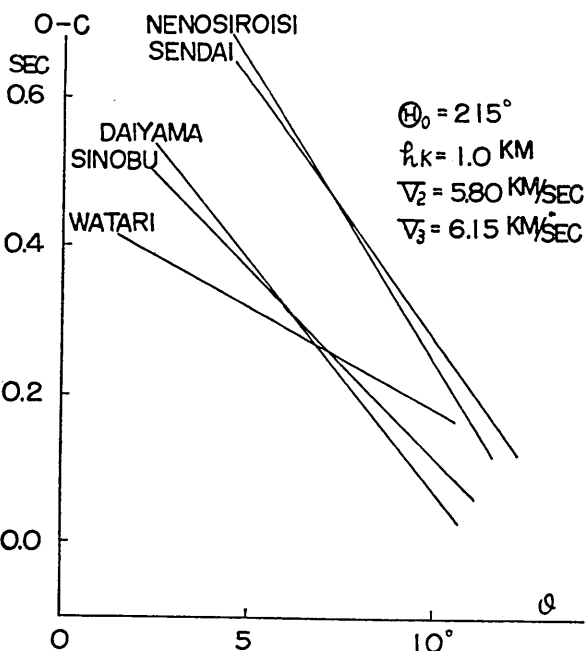


Fig. 22.

tion of the layer is situated at some distance in the west and its depth is small.

For case (a) one example of the relation between θ and h_k is given in Fig. 23.

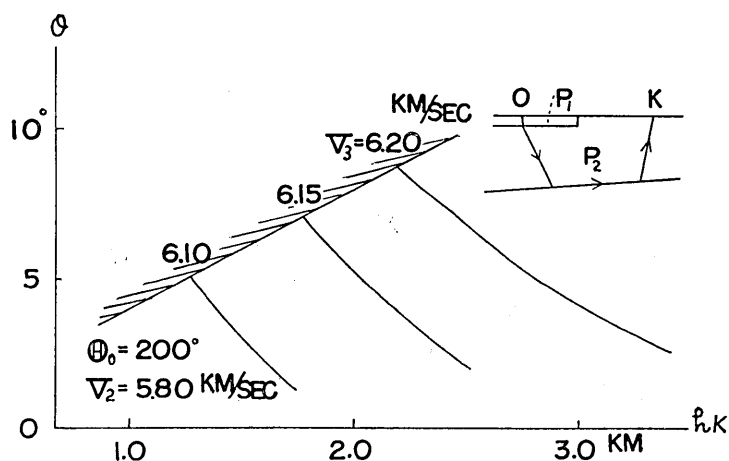


Fig. 23.

In the upper hatched domain P waves through P_3 layer cannot reach Kamaisi station. The calculated θ turns out too small, judging

from other data, and untenable.

For (b) θ and V_3 relation is shown in Fig. 24.

The domain of θ for existence of case (b) is above 3.5° .

It is remarked that the incident time of the first phase at Kamaisi is read 14.84 sec in this investigation instead of 15.33 sec in the 1.2⁴⁾ report. The latter value is interpreted as a late phase.

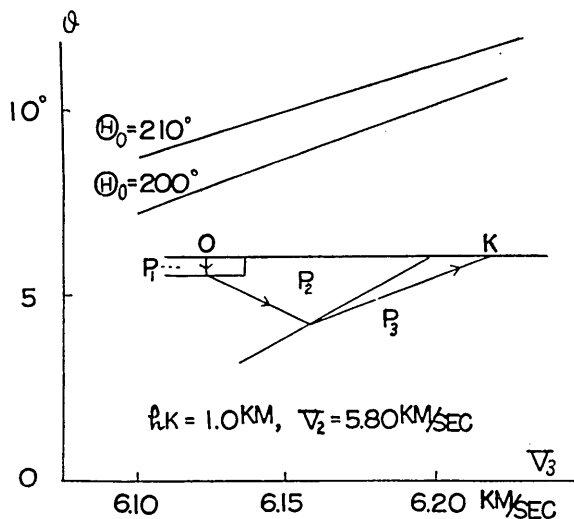


Fig. 24.

4) Research group for explosion seismology, B.E.R.I., 30 (1953), 279.

(vii) *In the KS profile*

In this profile, all stations are nearly on azimuth $\theta=200^\circ$, and moreover even at nearby stations waves through the P_3 layer appear. Therefore, the variation of θ does not affect much other parameters. Putting $\theta_0=200^\circ$, $\theta=10^\circ$ and $V_2=5.80$ km/sec, h_k calculated from various stations with V_3 as parameter is tabulated in Table 9.

Table 9.

Station V_3	Nakasone	Setamai	Sakari	Kesen- numa	Sizu- gawa	Ona- gawa	Mukai- yama	Huna- oka
6.15	2.3	2.1	2.8	2.3	2.7	2.9	3.5	3.5
6.20	2.4	1.9	1.9	2.0	2.9	2.1	4.9	2.7

In this calculation, the effect of a superficial layer on the travel time is not taken into account. Hence, the real h_k cannot be larger than the above shown value, namely it must be smaller than 2.0 km.

In (iii) we put an upper limit to θ from the intercept time. Here we can also put a limit to θ from h_k and h_1 .

(viii) *Summary on the form of the boundary between the P_2 layer and P_3 layer.*

Summarizing the above discussions we can put limits to the range of variation for θ_0 , θ , h_k , V_2 and V_3 , so that the error of travel time does not exceed 0.1 sec. Table 10.

Table 10.

Parameter		Range of allowance
strike	θ_0	$200^\circ \sim 210^\circ$
Dip	θ	$6^\circ \sim 11^\circ$ (downward to the west)
Depth at Kamaisi	h_k	0.75~1.5 km
Velocity in layer	P_2, V_2	5.75~5.85 km
"	P_3, V_3	6.10~6.20 km

It must be remarked that we do not say that any combination of these five quantities within the given limits is allowable. For instance, we will give an example of the allowable range for θ , giving certain definite values to other parameters (Fig. 25).

In case (a) we can choose a common range of θ , $9^\circ \sim 10^\circ$, compatible

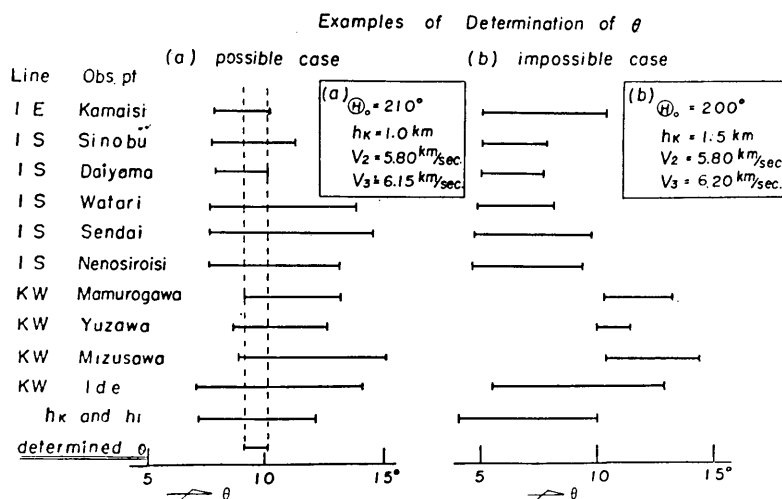


Fig. 25.

for all stations. In case (b) we cannot choose such a common range, and thus such a combination should be rejected.

After all, the range of allowance given in Table 10 is the broadest one within which the compatible range of each parameter falls for some choice of other parameters within their above given range.

(ix) *Consideration from reflected waves*

In profile KW seismograms with 11 elements were obtained at Umanokiuti for the purpose of obtaining reflected waves. On the record very distinct reflected waves can be seen about 0.1 sec after each initial phase. The travel time is given in Fig. 26.

If we take these phases for waves reflected at the P_2P_3 boundary, h_k turns out 0.3~0.7 km.

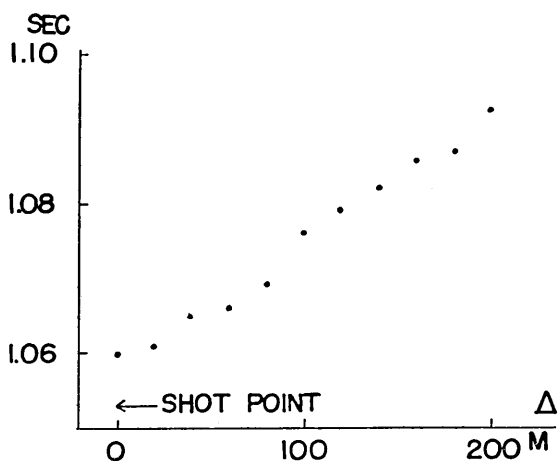


Fig. 26.

(x) *Consideration from late phases*

The most distinctly ob-

served late phase due to waves through P_2 layer in the IE profile is that at Kamaisi. As stated in (vi) this phase was taken for the initial phase in I.2 report⁵⁾. The path for this phase is expected to be as shown in Fig. 27.

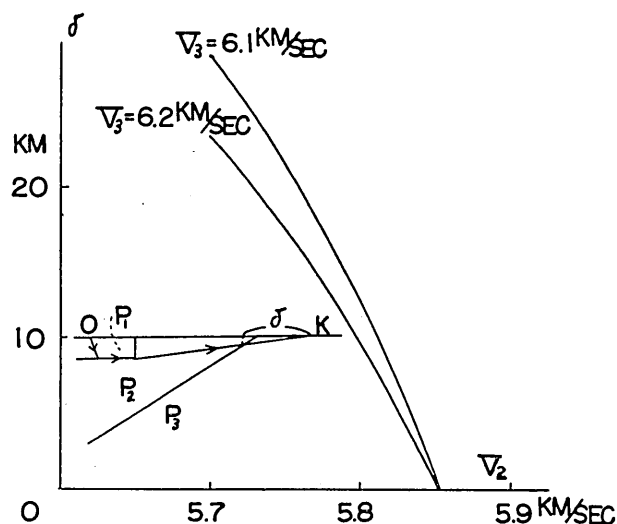


Fig. 27.

Length δ of a part of this path, i.e. the part in P_3 layer, can be calculated from its travel time. Taking V_3 as a parameter, the relation between δ and V_2 is shown in Fig. 27. As apparent from the figure, about 10 km is probable.

In other profiles, late phases expected to be due to waves through P_2 layer are observed at Sendai, Daiyama, and Sinobu for Isibuti explosions and at Sizugawa, Onagawa, Mukaiyama, Hunaoka, Kaneyama, and Kawamata for Kamaisi explosions. These facts will serve as other confirmatory evidences for the existence of the P_2 layer at least under these regions.

(xi) *The P_4 layer*

As stated in section 6, travel times corresponding to velocity 7.5~8.0 km/sec are distinguished at stations beyond 160~170 km on both IS and KS profiles. A graph for $T-(\Delta/8)$ and Δ is shown in Fig. 28.

The intercept time is about 5~6 sec. This fact reveals the existence of a layer, say P_4 , under the P_3 layer. This layer may correspond

5) *l. c.* (4)

probably to the so-called P_n layer, because of the velocity.

Travel times are not on a straight line, but fluctuate around it.

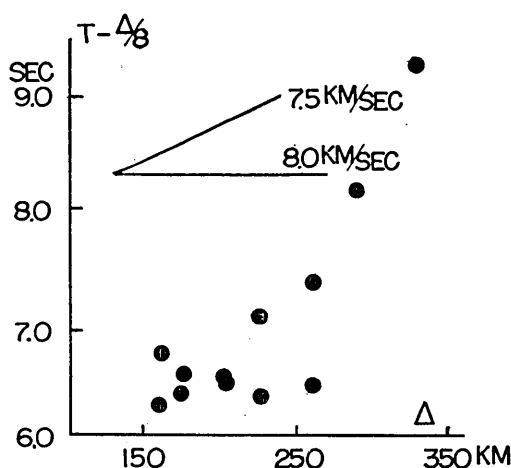


Fig. 28.

The exact form of the upper boundary of the P_4 layer cannot be discussed as precisely as was done in section (vi), because at stations beyond $\Delta=150$ km the initial motion was sometimes obscure and a few readings were not accurate enough for the purpose. Therefore, in this stage it may be wise not to make the attempt. As a rough approximation we assume a horizontal boundary and calculate its depth for some allowable values of V_2 , V_3 and V_4 , using

the intercept time and neglecting the existence of the P_1 layer, as its effect is negligible in this case (Table 11).

Table 11.

Profile	V_2	V_3	V_4	depth of layer P_4
IS	5.8	6.2	8.0	24
KS	5.8	6.2	8.0	24
IS	5.8	6.1	7.5	21
KS	5.8	6.1	7.5	22
IS	5.8	6.1	8.0	20
KS	5.8	6.1	8.0	23

Thus, probable ranges of the apparent depth of the layer and the apparent velocity in it can be taken as 20~25 km and 7.5~8.0 km/sec respectively.

(xii) Consideration from reflected waves

In the case of the K.2 explosion a reflected phase with travel time 7.33 sec was observed at Umanokiuti. As stated in 10 (ix), the depth of the P_2P_3 boundary under this station is very small. Thus, it is very probable that these reflected waves are due to the P_3P_4 boundary. Using

the relation $TV_3/2 = \sqrt{\Delta^2/4 + h^2}$, where T is the travel time, V_3 the velocity in layer P_3 , Δ the epicentral distance of Umanokiuti and h the depth of the boundary, we get $h=22\sim 23$ km. This value is not affected much by the surface correction, and nearly equal to the value obtain in (xi).

11. Summary on the Crustal structure of this area

Summarizing the above discussions, we obtain a broad aspect of crustal structure of this area. This has already been given in R.A.R., however, we repeat it here again.

The crustal structure of this region consists of the following 4 layers.

Layer	P_1	velocity	2.51 km/sec
	P_2		5.75~5.85 km/sec
	P_3		6.1 ~6.2
	P_4		7.5 ~8.0

Pattern of stratification of each layer is as follows.

(1) The P_1 layer is about 530 m deep near Isibuti and inclined at 9° ca. toward the east.

(2) The P_1 layer ends abruptly at a point 14 km east from Isibuti. In the further east near Mizusawa and Umanokiuti a thin surface layer is found.

SCHEMATIC ILLUSTRATION OF CRUSTAL STRUCTURE IN THE AREA.

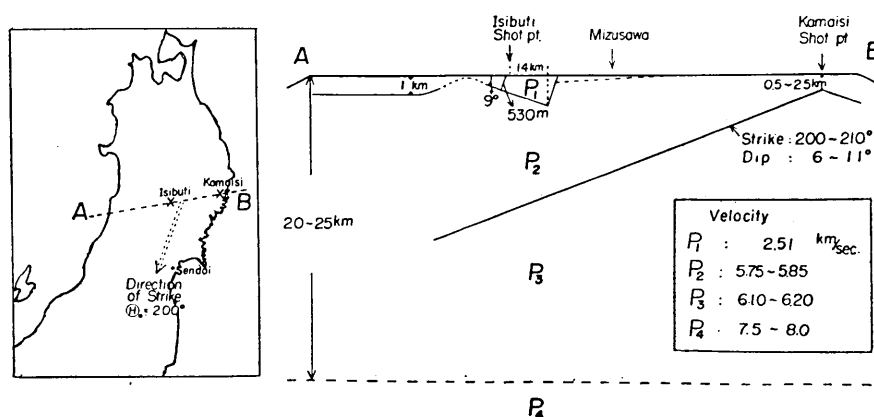


Fig. 29.

(3) In the west near Isibuti the P_1 layer is very thin or lacking. Further west, however, it again takes a depth of about 1 km.

(4) Near the Kamaisi shot point the P_1 layer is not found.

(5) South of the Isibuti shot point the P_1 layer is found, but its exact form is not known.

(6) The boundary between the P_2 and P_3 layers is probably a plane with strike $200^\circ \sim 210^\circ$, and dip $6^\circ \sim 11^\circ$ downward to the west.

(7) The depth of the P_1 layers turns out to be $20 \sim 25$ km, if it is taken as horizontal.

A general view of the east-west cross section is given in Fig. 29.

Observations of four smaller blasts were made at the east edge of the area studied. A brief sketch of the results was given also in R.A. R., but the details are described in a separate paper⁶⁾.

12. Comparison with gravimetry and surface geology

(i) From gravimetry

From the Bouguer anomaly of the gravity given by C. Tsuboi⁷⁾, A.

Jitsukawa, and H. Tajima, Fig. 30, giving those between Isibuti and Kamaisi, is obtained.

On the other hand, assuming the density difference $\Delta\rho$ between P_2 and P_3 layer as $0.05 \sim 0.15$, the Bouguer anomaly expected from our subterranean structure is shown in Fig. 31.

Comparing these figures, we see that the observed anomaly can be at least partly explained by our model.

A line connecting the steepest horizontal gradient of Bouguer anomaly in the Tōhoku District, namely Morioka-Sirakawa line of C. Tsuboi

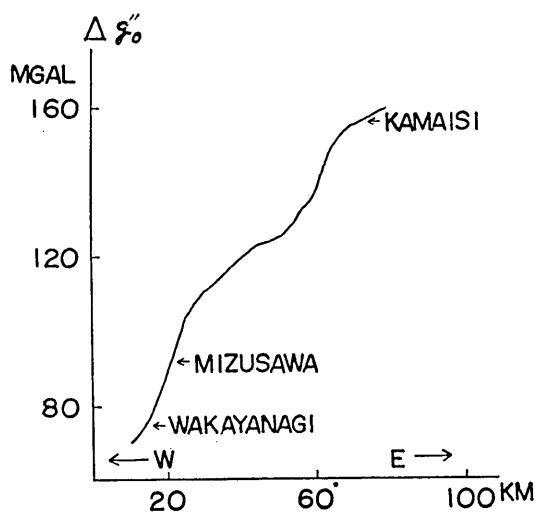


Fig. 30.

6) Research group for explosion seismology, *Bull. Earthq. Res. Inst.*, **37** (1959).

7) C. TSUBOI, A. JITSUKAWA and H. TAJIMA, *Bull. Earthq. Res. Inst., Suppl. Vol. 4* (1956), 311-406.

et al., has also nearly the same azimuth as the strike of the P_2P_3 boundary as stated in section 11 (6).

(ii) *From surface geology*

Geological structure in the east-west cross section passing Isibuti and Kamaisi inferred from the surface geology is schematically given in Fig. 32.

In the neighbourhood of Isibuti shot point a tertiary layer extends eastward, but it is lacking at Mizusawa. Along the back bone mountain range it is very thin and further west it increases again in depth.

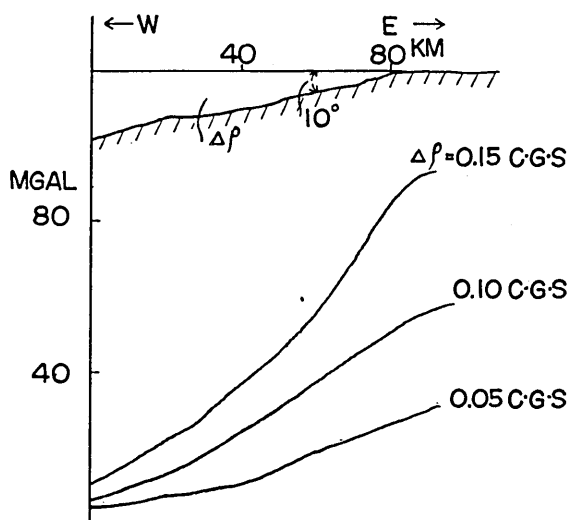


Fig. 31.

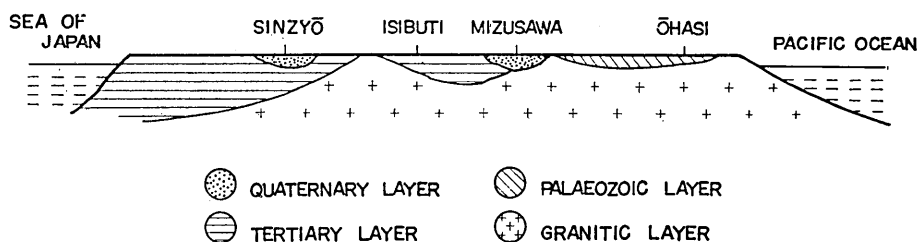


Fig. 32.

The Kitakami mountain range is covered from place to place with thin palaeozoic strata, but its main body is supposed to consist of granitic rocks. Patches of granitic rocks are found on the back bone range and they are supposed to be akin to those in the Kitakami range.

Basins at Mizusawa and Sinzyō are covered by a quaternary layer.

Comparing these geological data with our model, it seems very probable that our P_1 layer corresponds to the tertiary layer and P_2 layer to the granitic base.

Further comparison in some detail will be given below.

(i) Palaeozoic strata on the Kitakami mountain range are omitted in our model. It means their trivial thickness.

(ii) Abrupt disappearance of the P_1 layer at 14 km east from the Isibuti shot point may correspond to a NS fault line shown on a geological map, though its exact position is shifted somewhat eastward.

(iii) As for the P_3 layer, we have no direct geological evidence in this area. However, patches of ultrabasic rocks are exposed from place to place on the Kitakami range, but they are scarcely found westward from Mizusawa. This fact makes us suppose that their source should be shallower in the east. This parent rock may probably correspond to our P_3 layer.

After all, our model does not contradict the geological knowledge in this area, and we may say that the correspondence is rather good.

13. Acknowledgement

At every set of observations, which constitute the basis of our present discussions, we got kind cooperation of inestimable value from many institutions, organizations, and authorities, for which we are much obliged. They were mentioned in each case in our previous publications, so that we may be allowed not to repeat them here.

Our sincere thanks are due to Professors Kenzo Yagi, Tadamasa Sendo, Iwao Kato, Yoshio Onuki, Yoshio Ueda, Asahiko Sugaki, Ryohei Morimoto and Masao Minato for their kind advice and instructions from the geological and petrological point of view.

Financial support for these works was partly granted from the research fund for sciences of the Ministry of Education and much explicit and implicit help was given by organizations to which our participant members belong.

Last, but not the least the present writer is much obliged to Mr. S. Asano for his devotedly sincere cooperation in preparing this paper and to Miss Yoriko Utida, who prepared many text figures in a short time.

7. Bakuha-Zisindô ni yoru Tôhoku-Tihô no Tikaku no Kôzô.

Tôkyô-Daigaku Rigakubu, Tikyû-Buturi-gaku Kyôsitu,

MATUZAWA-Takeo.

Isibuti 3 Kai oyobi Kamaisi 2 Kai no Daibakuha Zisindô no Kansoku wo subete kangaeawasete mitibiki dasita Tikaku no Kôzô ni tuite no Aramasi wa 1954 nen no Roma no I.U.G.G. Kaigi no Hôkoku ni dete iru. Koko dewa sorera wo mitibiki dasu Toki ni okonatta Keisan naisi wa Kenkyû no Tedate ni tuite kuwasiku nobete aru.